Photoluminescence Properties of a Perfluorinated Supramolecular Columnar Liquid Crystal with a Pyrene Core: Effects of the Ordering and Orientation of the Columns

Yun Ho Kim, Dong Ki Yoon, Eun Ho Lee, Young Koan Ko, and Hee-Tae Jung*

Department of Chemical and Biomolecular Engineering (BK-21), Korea Advanced Institute of Science and Technology, 373-1 Guseong-dong, Yuseong-gu, Daejeon 305-701, Korea

Received: May 22, 2006; In Final Form: July 24, 2006

We investigated the effects of the alignment and ordering of π-conjugated perfluorinated dendrimers containing pyrene moieties in their cores on their photoluminescence (PL) properties. The pyrene molecules are stacked in columns surrounded by aromatic and semifluorinated tails, which can be conjugated and act as chromophores. Polarized light microscopy (PLM), cross-sectional scanning electron microscopy (SEM), and atomic force microscopy (AFM) results show that variation of the cooling rate of the dendrimers produces variation in their orientation and ordering: Slow cooling ($\sim<0.5$ °C/min) of the isotropic melt in a sandwich glass cell results in a high degree of ordering and the vertical alignment of the columns on the substrate, in which the stacked pyrene molecules are oriented parallel to the surface over large areas. In contrast, rapid cooling ($\sim>10$ °C/min) leads to the planar alignment of the columns with significant disorder on the same substrate. UV−vis, PL, SEM, and AFM results show that the quenched columns with a planar orientation produce a broad emission band and a second weak shoulder, which indicates the presence of isolated molecules. However, the high degree of ordering of the columns with a vertical alignment produces a red-shift in the PL spectrum, with very few isolated molecules. By comparing two films with different alignments but similar ordering, we show that the ordering of this material has a greater influence on the PL spectrum than the alignment. This effect of the ordering of the columns was further verified by comparing the optical properties of the isolated dendrimers with those of small π-conjugated molecules in solution and solid films.

Introduction

π-Conjugated supramolecular dendrimers have attracted considerable attention because of their potential applications in light-emitting diodes (LEDs),[1,2] field-effect transistors (FETs),[3,4] and electroluminescent (EL) devices.[5−7] As with all other types of nanostructured materials,[8,9] control of the supramolecular ordering and orientation of the π-conjugated dendrimers is crucial to such applications. Previous research into small π-conjugated molecules and polymers has shown that their optoelectronic properties are strongly affected by the alignment of their π-conjugated elements. For instance, LB monolayers of poly(*p*-phenyleneethynylene)s (PPEs) exhibit edge-on, face-on, alternating face-on, and edge-on (zipper) orientations depending on their chemical structures and surface pressures.[10] A large blue-shift was found to be generated by the transition from the face-on to zipper alignment. This shift occurs because the interlocked zipper structure lacks extended π-conjugation and so has a reduced exciton diffusion length and reduced quenching. Moreover, it has been reported that the field-effect mobility in magnetically aligned films of substituted hexabenzocoronene (HBC), in which the molecular columns are aligned perpendicularly to the magnetic field and individual HBC molecules are aligned along the magnetic field in an edge-on arrangement due to paramagnetism, is ~10 times higher than that in isotropic films.[11] Further, alignment layers of rubbed poly(vinyl alcohol) or irradiated cinnamic self-assembled monolayers (SAMs)[12,13] induce preferential orientation of pentacene grains along the rubbing direction, leading to an enhancement of pentacene mobility.

Little research has been carried out into the effects of alignment and ordering of π-conjugated supramolecular dendrimers on their optoelectronic properties, largely due to the difficulty of designing and aligning such materials on the surfaces of interest. Our interest in the control of the long-range order and orientation of fan-shaped supramolecular columns led us to investigate the effect of the ordering and alignment of π-conjugated supramolecules on their photoluminescence (PL) properties.[16] It has recently been reported that perfluorinated supramolecular building blocks containing conjugated donor and acceptor dendrons self-assemble into columnar mesophases and exhibit a 2−5 orders of magnitude increase in their charge-carrier mobility over that of amorphous polymers.[14,15] These compounds form π-conjugated systems in the inner core, and this chromophore core lends structural stability to these compounds. Moreover, the semifluorinated tails encapsulate the conjugated inner core cylinder by forming an "envelope" that protects its photoexcited state from self-quenching.[16] However, determining the effects of the ordering and orientation of these types of materials on their optical properties is challenging and has not yet been reported, despite their potential applications in sensors, light-emitting displays, lasers, and solar cells.[17−19] In this study, we demonstrated that perfluorinated supramolecular columnar liquid crystals containing a pyrene core and three semifluorinated tails exhibits PL properties in solution and in the solid state. The columnar alignment of the molecules is indirectly manifested in the photophysics of the pyrene moieties at their cores. Cross-sectional SEM images, PLM, AFM, UV−

* To whom correspondence should be addressed. Phone: +82-42-869-3931. Fax: +82-42-869-3910. E-mail: heetae@kaist.ac.kr.

10.1021/jp063115j CCC: $33.50
Published on Web 09/28/2006

SCHEME 1: Homeotropically Aligned Hexagonally Packed Cylinders of 1 in a Sandwich Cell

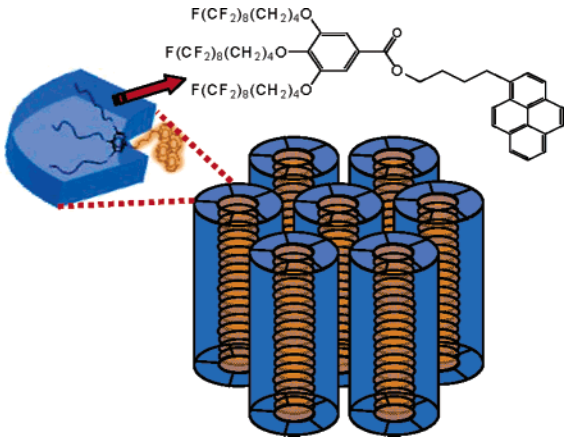

vis, and PL results show that the emission properties of the semifluorinated dendrimers are strongly influenced by the ordering of the supramolecular columns in thin films, whereas the alignment of the columns has little effect.

Experimental Section

Materials. The fan-shaped supramolecule used in this study (Scheme 1), which contains a pyrene core and semifluorinated tails, was synthesized as described previously.[14,20] Compound **1** [4-(1-pyrenyl)butyl]3,4,5-tris(12,12,12,11,11,10,10,9,9,8,8,7,7,6,6,5,5-heptadecafluoro-*n*-dodecan-1-yloxy)benzoate was synthesized by the esterification of 3,4,5-tris(1*H*,1*H*,2*H*,2*H*,3*H*,3*H*,4*H*,4*H*-perfluorododecan-1-yloxy)benzoic acid and 1-pyrenebutanol. TLC: R_f = 0.52 (CH_2Cl_2/hexanes, 2/1). ^{1}H NMR ($CDCl_3$, 300 MHz, 20 °C): δ 8.26 (d, 1H, J = 7.6 Hz), 8.18−7.98 (m, 7H), 7.89 (d, 1H, J = 7.8 Hz), 7.24 (s, 2H), 4.4 (t, 2H, J = 6.0 Hz), 3.98 (m, 6H), 3.44 (t, 2H, J = 7.3 Hz), 2.13 (m, 8H), 1.81 (m, 14H). The following reagents were used: methyl *p*-hydroxybenzoate (99%), K_2CO_3 (99+%), methyl 3,4,5-trihydroxybenzoate (98%), lithium aluminum hydride ($LiAlH_4$) (95%), CH_2Cl_2 (99.9%, ACS reagent), *N*,*N*-dimethyl formamide (DMF) (99.8%, ACS reagent), ethyl alcohol (99.5+%), 1,1,2-trichloro-1,2,2-trifluoroethane (Freon 113) (99.9%), 1.3-dicyclohexylcarbodiimide (DCC) (99%), 1-pyrenebutanol (99%) (all from Aldrich); methanol (ACS reagent, from Merck); $SOCl_2$ (99.0+%, from Fluka); KOH (from Junsei). Tetrahydrofuran (THF) (99.0%, Junsei) was distilled by refluxing over CaH_2 prior to use. Silica gel (grade 60, 230−400 mesh ASTM) (from Merck) was used for column chromatography. Teflon AF (from Dupont) in FC-77 (from 3M) solution was used for hydrophobic treatment of the substrates.

Sample Preparation. To obtain homeotropically aligned samples, we used sandwich cells with two glass or quartz substrates. The cells were assembled by cementing the two substrates together, separated by silica microbeads with 10 μm spacers. These cells were then filled in the isotropic phase using the capillary effect and then slowly cooled to the liquid crystalline phase at various cooling rates from more than 30 °C/min to 0.1 °C/min. The cell thickness was controlled by the silica bead spacers at 10 μm. To obtain cross-sectional SEM images, the two substrates were precut with a glass knife and immersed in liquid nitrogen with the appropriate stress. Each cell was cut normal to the surfaces, and the cross-sectional surface was coated with about 30 nm vacuum-evaporated platinum for high resolution. For the AFM specimens, thin films of supramolecules on the fluorinated (Teflon-AF) substrates were cast from a solution of 1 wt % in THF onto distilled water. These thin films of thickness ~50 nm were slowly cooled to the liquid crystalline phase at 0.1 °C/min. To improve the mass contrast and radiation sensitivity, the thin films were exposed to RuO_4 vapor (solutions of 0.5 wt % aqueous RuO_4) for 3 min.[21]

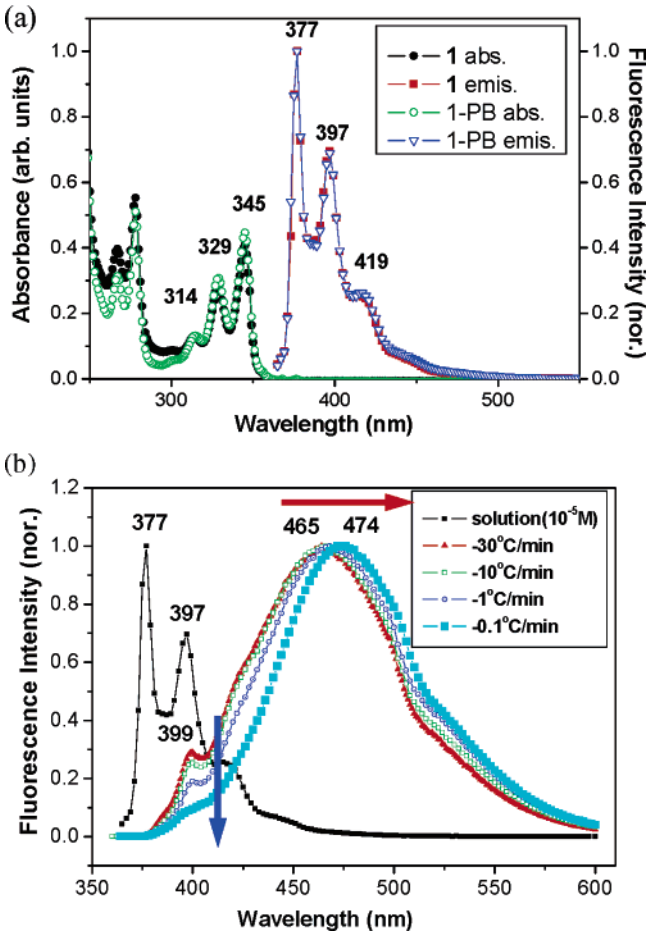

Figure 1. (a) Absorption and PL spectra of compound **1** and 1-pyrenebutanol in chloroform (10^{-5} M). (b) Solid films produced by introducing **1** into a sandwich glass cell using the capillary effect and then slowly cooling the cell to the liquid crystalline phase at various cooling rates from more than 20 to 0.1 °C/min. The spectra have been normalized to maximum intensity; the PL spectra were measured by excitation at 345 nm.

Techniques. ^{1}H NMR (300 MHz) spectra were recorded on a Bruker DRX-300 FT-NMR spectrometer. DSC experiments were carried out with a Perkin-Elmer DSC-7 with heating and cooling rates of 5 °C/min. XRD measurements with a synchrotron beam source were performed in transmission mode at the 3C2 and 4C2 X-ray beam lines with λ = 0.154 nm at the Pohang Light Source (PLS), by using the 2.5 GeV LINAC accelerator. A polarized optical microscope (Leica, DMLB) equipped with a hotstage (Mettler FP82) was used to analyze the columnar phase textures and determine $T_{\phi h}$ (the hexagonal-to-isotropic transition temperature). Cross-section images and the surface morphologies were obtained at various magnifications using a field emission scanning electron microscope (Serion FE-SEM, FEI) equipped with a Schottky-based field emission gun. The surface topological measurements were performed under ambient conditions using AFM (SPA 400 microscope, Seiko Instruments). The silicon cantilevers of an SI-DF20S (dynamic force mode) were used for the condensed phase. UV−vis spectra were recorded on a Cary-Varian at room temperature using a 10 mm quartz cell and a solute concentration of 10^{-5} M in chloroform

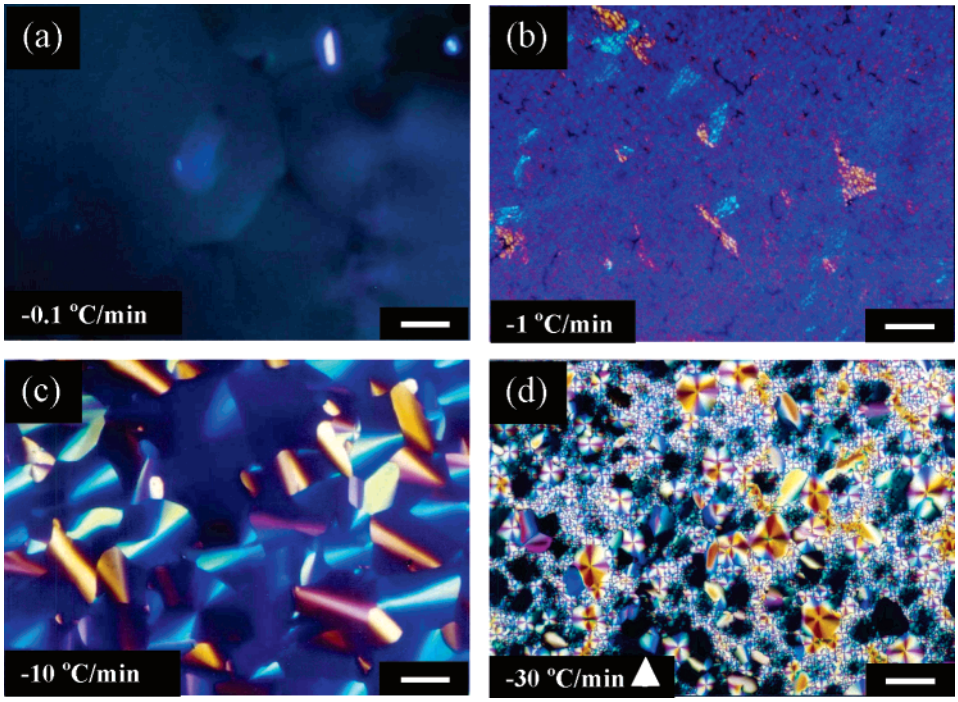

Figure 2. POM images of films of **1** produced with various annealing rates in sandwich cells with all images obtained at room temperature. The cooling rate gradually decreases from (a) to (d). Note that the slower the cooling rate, the larger the domain size and the more efficient the molecular packing. (a) For slow cooling (0.1 °C/min), a vertically aligned structure is obtained with large domains. (d) For fast cooling (>30 °C/min), a randomly planar spherulite-like structure is obtained with small domains. The scale bar is 100 μm in length.

for the solution measurements. PL spectra were recorded on an ISS PC1 spectrofluorometer using a 10 mm quartz cell and a solute concentration of 10^{-5} M in chloroform. The films for the PL spectra were prepared in sandwich cells of 10 μm thickness between two quartz slides.

Results and Discussion

The fan-shaped supramolecule used in this study, which contains a π-conjugated pyrene unit in the core and semifluorinated tails, was synthesized by the esterification of 3,4,5-tris(1*H*,1*H*,2*H*,2*H*,-3*H*,3*H*,4*H*,4*H*-perfluorododecan-1-yloxy)-benzoic acid and 1-pyrenebutanol. The synthetic procedure has been previously described in detail.[20,22] There has been much recent interest in studying the microstructure and properties of perfluorinated supramolecular columnar materials, since they have greater enhanced mesophase stability on account of the presence of strong intermolecular interactions that promote and enhance the microphase separation of the hydrophobic perfluorinated tail groups and the polar core segments. Various core molecules, which interact with other molecules via hydrogen-bonding interactions and other noncovalent interactions while also providing a covalent backbone along the core, have been used in complex functional materials.[14] The chemical structure of the dendrimer and a schematic representation of its self-organization are shown in Scheme 1. Our synchrotron X-ray diffraction (XRD), differential scanning calorimetry (DSC), and PLM results show that this dendrimer exhibits a hexagonal columnar mesophase (with lattice parameter $a = \sim$4.5 nm) upon cooling from the isotropic temperature (see the schematic illustration of the overall synthetic procedure, sample preparation, and characterizations in the Supporting Information).

To investigate the role of the pyrene in the photoluminescent core, we compared the UV−vis absorption and emission spectra of the dendrimer with those of a small 1-pyrenebutanol molecule in dilute solution. The absorption and emission spectra of the dendrimer in dilute solution (chloroform, 10^{-5} M) are very similar to those of 1-pyrenebutanol (Figure 1a). The UV−vis absorption spectra of both compounds indicate there is coupling of the vibronic features corresponding to $\nu = 0$ to $\nu' = 0, 1, 2$ transitions, where ν and ν' are the quantum vibrational numbers of the ground and excited states, respectively. The emission maxima centered at 377, 397, and 419 nm are attributed to the vibrational peaks of the pyrene momoner,[23] indicating that the pyrene group is responsible for the luminescent core within the dendrimer architecture. It is notable that similar PL behavior was obtained for other perflorinated dendrimers containing pyrene cores and semifluorinated tails (Supporting Information). We also investigated the variation of the PL spectra of a solution of the dendrimer in chloroform with concentration (see Supporting Information). Increasing the dendrimer concentration yields an increase in the relative absorption intensity of the 0 → 1* and 0 → 2* transitions, because the Franck−Condon factor $\langle\chi_{1'}|\chi_0\rangle$ increases faster than $\langle\chi_{0'}|\chi_0\rangle$.[24] Thus, the emission vibrational overlap integral $\langle\chi_{0'}|\chi_{\nu}\rangle$ favors radiative transitions to higher and higher ground vibronic states ($\nu = 0, 1, 2$) with increases in the degree of self-aggregation of the dendrimer. Thus, as the size of the aggregate increases, the emission shifts toward the red. Previous experimental and theoretical works have concluded that face-to-face stacking interactions in aromatic π-systems result in an increase in the intensity of the 0* → 1 and 0* → 2 transitions and in turn lead to a red-shift of PL spectra.[25]

Very different PL properties were observed for thin films of the π-conjugated supramolecular columnar liquid crystal (Figure 1b). The films were prepared for the PL experiment by filling the space between two quartz substrates with isotropic samples. The samples were heated to the isotropic temperature (with a Mettler FP82 hotstage and a Mettler FP90 controller) within the sandwich quartz cell separated by 10 μm thick spacers (silica microbeads). Interestingly, the PL properties are strongly affected by variation of the rate of cooling from the isotropic temperature. PL spectra of the thin films prepared using different

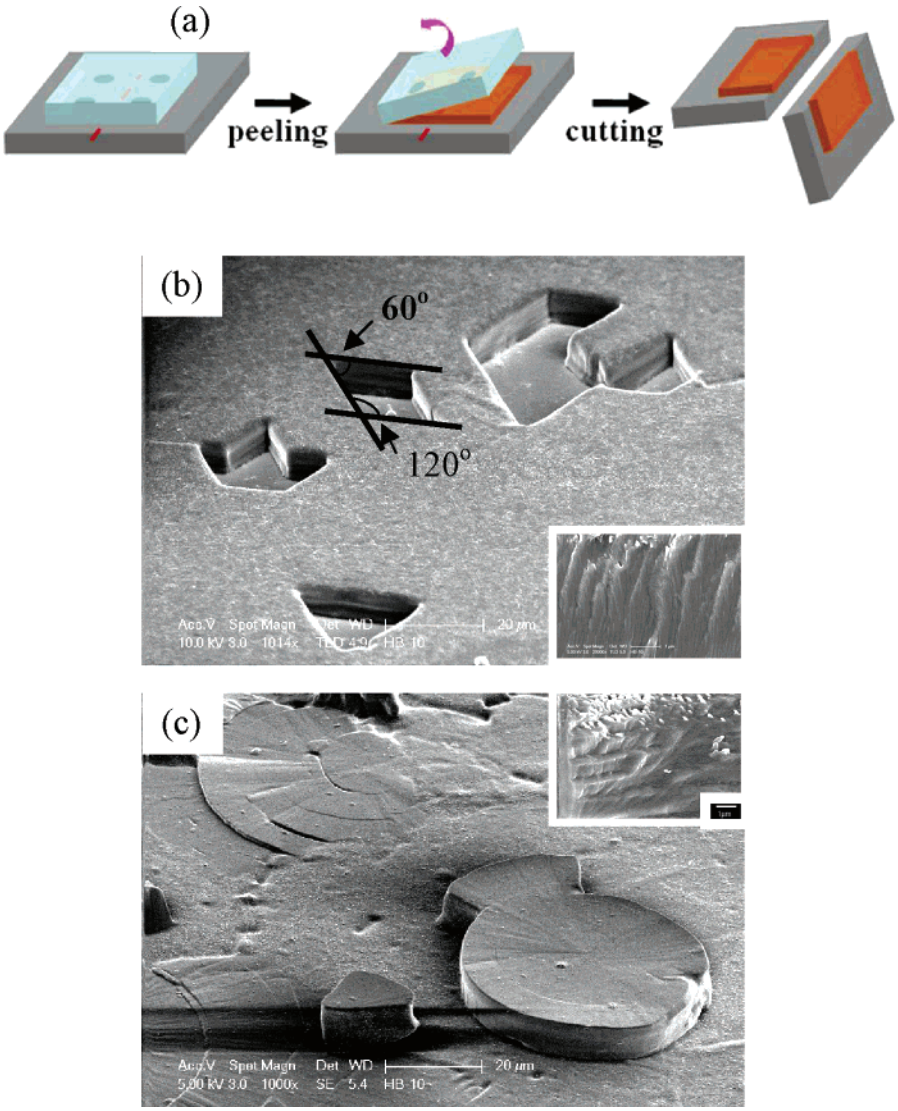

Figure 3. (a) Preparation of the thin film for cross-sectional SEM observations. Cross-sectional samples for an SEM micrograph of fragments of thin film are made by impact to the films in liquid nitrogen. (b) Traces of fragments of homeotropically aligned hexagonal cylinders at slow cooling (0.1 °C/min) conditions. The inset shows homeotropic alignment. (c) Real fragments of planar layered cylinders grown by nucleation mechanisms at rapid cooling (>30 °C/min) conditions. The inset shows randomly planar alignment; these images were obtained by tilting the holder by 52° at room temperature.

cooling rates show the existence of intermolecular electronic interactions, indicating a tight-packing geometry of π-stacked molecules (Figure 1b). Moreover, the PL spectra in the solid films become increasingly red-shifted as the cooling rate decreases. Superposition of several different excited states occurs because of the excimer state and is broader than in the solution spectrum as a result of the fluorescence quenching effect.[26,27] As the cooling rate is decreased from 30 to 0.1 °C/min, a ~10 nm red-shift in the emission peak of λ_{max} of the PL spectrum is observed. A weak shoulder peak maximum at 399 nm corresponding to isolated dendrimer molecules is also observed in the spectra of the films, as shown in Figure 1b. As the cooling rate is decreased, however, the normalized peak intensity at 399 nm is progressively reduced. Longer wavelength emission (approximately 470 nm) becomes more prominent due to excimer emission, since the higher energy photons emitted by weakly conjugated molecules are increasingly reabsorbed or quenched as the conjugation of the chromophore increases.[28] The PL spectra of the solid films produced with a cooling rate of 0.1 °C/min are similar to that of pyrene crystals, indicating the occurrence of structureless excimer emission without any monomer emission.[29] When a pyrene crystal absorbs light, two parallel pyrene molecules have a tendency to move toward one another and toward more complete overlap.[30] Thus, under slow cooling conditions, the pyrene chromophores in the center of the supramolecular columns are strongly conjugated, as arises in the pyrene crystal structure. On the other hand, the PL spectra of the quenched samples contain a weak vibronic shoulder peak at 399 nm (the $0^* \rightarrow 1$ transition of the monomer), perhaps because of imperfect overlapping of the π-electrons in the pyrene chromophore.

To elucidate the effect of changing the cooling rate on the PL spectra of the solid state, we investigated the variation with cooling rate of the morphology of the solid film. Interestingly, both the ordering and the alignment of the columns were affected by variation of the cooling rate. Figure 2 shows PLM textures of the compound in sandwich glass cells for various cooling rates. On cooling (10 °C/min) of the sample from the isotropic phase, fan-shaped domains arise in the solid films (thickness ~10 μm), which is a characteristic texture of columnar mesophases (Figure 2c). The domain size of the fan-shaped PLM textures was found to decrease with increases in the cooling rate. However, no specific birefringence was observed a few degrees below the isotropic temperature on slow

cooling (~0.1 °C/min) from the isotropic phase (Figure 2a), indicating homeotropic alignment of the hexagonal cylinders. Over large areas of the sample, the columns are likely to be perpendicularly oriented to the surface, and there are a few disclinations where abrupt changes of orientation around disclinations of columns are observed.

Clear evidence of columnar alignment was also provided by the cross-sectional SEM images. For the SEM specimens, thin films in sandwich glass cells were prepared by freeze-fracture under a liquid-nitrogen atmosphere (Figure 3a). First, the sandwich glass cells were separated by 10 μm thick spacers (silica microbeads). The cells were filled by the capillary effect above the isotropic temperature and cooled to the liquid-crystalline phase at various cooling rates. The cells were then cross-sectioned and immersed in liquid nitrogen. The cells were cut normal to the surfaces, and the cross-sectional surfaces were coated with vacuum-evaporated platinum. For a slow cooling rate (0.1 °C/min), top views of the SEM traces show a specific angle of 60 or 120°, indicating that the assembled cylinders are packed hexagonally for geometric stability (Figure 3b). The hexagons have an interior angle of 120°, and each hexagon contains six regular triangles with internal angles of 60°. When a stress is applied to the films, the domain boundaries fragment, with the hexagonal geometry broken down into two or three components. The alignment is made clear by examination at higher magnification, which reveals homeotropic alignment with respect to the substrate (Figure 3b, inset). Note that the vertical alignment of the hexagonal columns spans the ~10 μm thick layers in the sandwich glass cells. The strong intermolecular interactions and fluorophobic effects induce this perfect homeotropic alignment of the columnar structure.[31,32] However, for rapid cooling (30 °C/min) the pieces have no specific angles, as shown in Figure 3c. The surface morphologies of the quenched films are spherulite-like and are comparable to the texture obtained at a much larger length scale with optical microscopy (Figure 2d) for a sample cooled from the isotropic temperature at a rate of approximately 30 °C/min. The columns are significantly bent near the core of the defect, which is closely related to the elastic constant of the material. Therefore, for slow cooling rates the molecules are ordered in large periodic structures with a homeotropic orientation with respect to the film surface. However, this is not the case for the mesophase for rapid cooling rates. As a result, the ordering and orientation of the supramolecular columns vary with the cooling rate.

Which of the ordering and alignment is more important for the PL properties of the columns? The dominant factor can be determined by comparing two films with different alignments but similar ordering. To do this, we fabricated films with a high degree of planar alignment, in which the column axis is parallel to the film surface, on Teflon AF-modified glass surfaces with a cooling rate of 0.1 °C/min. As previously reported, the orientation of the perfluorinated columnar dendrimers can be controlled by surface anchoring, resulting in a high degree of alignment as confirmed with transmission electron microscopy (TEM).[21] Figure 4b shows a high-resolution nonfiltered AFM image and the corresponding Fourier transform power spectrum (inset) for supramolecular columns on a surface coated with Teflon AF. The cylinders are coherently aligned and are elongated along the cylinder axis. The (10) spacing of the columns on the Teflon AF surface was estimated from the power spectrum to be 4.5 nm, which is consistent with the XRD measurements. The peripheral $-CF_3$ tails of the supramolecule, which make the dendrimer strongly hydrophobic, are probably in direct contact with the surface covered with Teflon AF

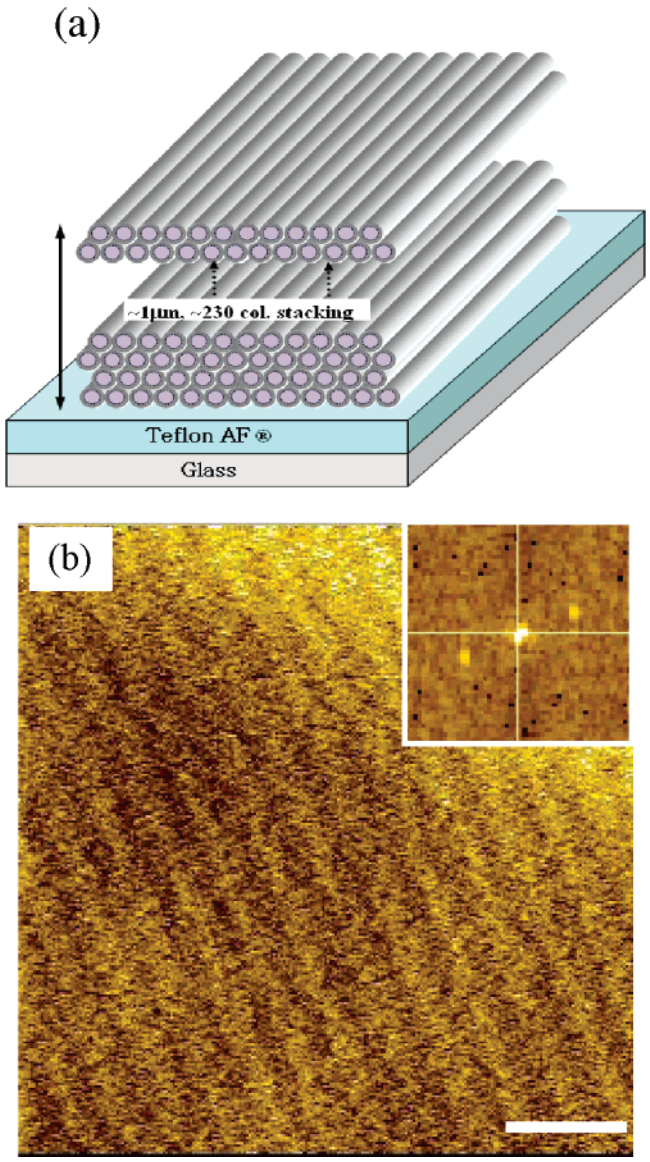

Figure 4. (a) Schematic representation of the planar-aligned Φ_h LC assembly produced by taper-shaped supramolecular columns on Teflon AF treated glass. This film has a thickness equal to approximately 230 column diameters (diameter is 4.5 nm). (b) AFM micrograph showing the planar orientation of the hexagonal cylinders on the substrate. A 60×60 nm^2 AFM image of the hydrophobic surface was treated with Teflon AF. The films were slowly cooled to the liquid crystalline phase at 0.1 °C/min. The scale bar is 10 nm in length.

because of the strong chemical affinity between the $-CF_3$ groups on the supramolecule tails and the $-CF_3$ terminal groups on the Teflon AF (Figure 4a).[21] Moreover, the dendrimer is highly microphase-separated around the center of the core group, and each single slice of the columns may be strongly associated with other such slices.[20,22] As a result, the core groups are oriented away from the substrate. The cylinders ultimately self-organize into a planar alignment, as was demonstrated with AFM (Figure 4b).

Figure 5 shows the PL spectra of two thin films, one with a high degree of homeotropic alignment and the other with a high degree of planar alignment. Although the two films have different alignments as a result of surface anchoring, their spectra are very similar. Figure 5 shows simple excimer spectra with peaks around 474 nm that are due to the perfect conjugation of the pyrene moiety, with no weak vibronic shoulder peak at 399 nm (the $0^* \rightarrow 1$ transition of the monomer), which is

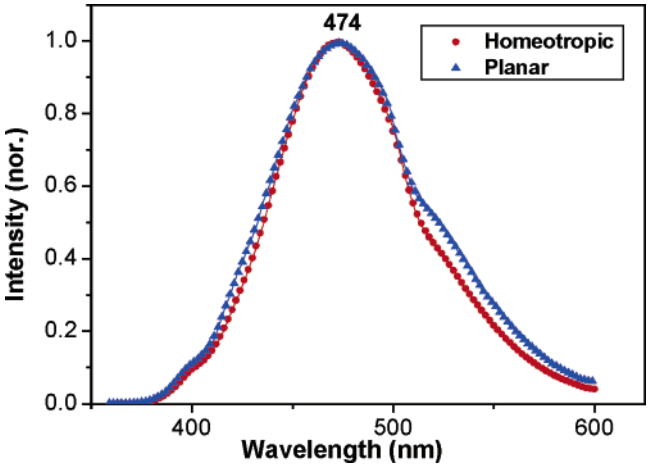

Figure 5. PL spectra of films with homeotropic and planar alignments. The PL spectra are similar to each other. The PL spectra were measured with excitation at 345 nm and normalized to maximum intensity.

characteristic of isolated molecules. Thus, the intensity of the excimer spectrum is dependent on the conjugation of the π-electrons in the columnar core rather than on the alignment of the columns; in other words, the ordering affects the conjugation length of the pyrene core in the center of column to a much greater extent than the alignment of the columns. In both the vertical and planar alignment cases when the columns are packed hexagonally, the π-electrons are highly conjugated in the cylinders. In contrast, the planar-aligned film with a spherulite-like structure that results from rapid cooling has imperfect π-electron conjugation. Therefore, the PL properties are strongly affected by the structural conjugation of the chromophore core, and the alignment of the columns has much less effect on the PL properties.

Conclusions

The aim of this work was to investigate the effects of the ordering and alignment of perfluorinated supramolecular columns containing conjugated cores on their PL properties. A synthetic semifluorinated supramolecule containing the pyrene group in its core was found to self-assemble into columns. This pyrene chromophore is a good probe for the investigation of the ordering and alignment effects because the self-aggregation is accompanied by a characteristic alteration of the PL spectra as a result of variation of the cooling rate of the solid film on the glass substrate. Slow cooling from an isotropic state results in a high degree of ordering and a vertical alignment of the columns with respect to the substrate in a sandwich glass cell and on the fluorine-treated (Teflon-AF) glass substrate, respectively, in which the π-conjugated molecules were efficiently packed together over large areas. In contrast, rapid cooling leads to planar alignment of weakly ordered columns on the same substrates. UV−vis and PL results show that less efficient packing of the π-conjugated molecules results in the production of a broad emission band and a second weak shoulder, which indicates the presence of isolated molecules. However, highly ordered columns with vertical and planar alignments produce excimer spectra that are typical of pyrene and a decrease in vibronic features due to isolated molecules. The fluorescence spectra of the material are attributed to the increase in the conjugation length that results from the formation of a cylindrical structure with perfect ordering. From the surface anchoring of the material, we conclude that ordering is a more important influence on the PL spectra of this material than alignment. To further define whether this effect of ordering on PL spectra is a general phenomenon, we are currently studying several supramolecules containing the pyrene chromophore.

Acknowledgment. This work was supported by the Basic Research Program of the KOSEF (Grant R01-2005-000-10456-0), CUPS-ERC, and KAIST initiative program. The Pohang Accelerator Laboratory is gratefully acknowledged for providing the 3C2 and 4C2 beam lines used in this study.

Supporting Information Available: A schematic illustration of the overall synthetic procedure, a description of sample preparation and characterizations, and PL spectra. This material is available free of charge via the Internet at http://pubs.acs.org.

References and Notes

(1) Friend, T. D.; Gyner, R. W.; Holmes, A. B.; Burroughes J. H.; Marks, R. N.; Taliani, C.; Bradley, D. D. C.; dos Santos, D. A.; Lögdlund, M.; Salaneck, W. R. *Nature* **1999**, *397*, 12.

(2) Sheats, J. R.; Antoniadis, H.; Hueschen, M.; Leonard, W.; Miller, J.; Moon, R.; Roitman, D.; Stocking, A. *Science* **1996**, *273*, 884.

(3) (a) Garnier, F.; Hajlaoui, R.; Yassar, A.; Srivastava, P. *Science* **1994**, *265*, 1684. (b) Horowitz, G. *Adv.* Mater. **1998**, *10*, 365. (c) Dodabalapur, A.; Torsi, L.; Katz, H. E. *Science* **1995**, *268*, 270.

(4) Yang, H.; Shin, T. J.; Yang, L.; Cho, K. W.; Ryu, C. Y.; Bao, Z. *Adv. Funct. Mater.* **2005**, *15*, 671.

(5) Halim, M.; Pillow, J. N. G.; Samuel, I. D. W.; Burn, P. L. *Adv. Mater.* **1999,** *11*, 371.

(6) Pillow, J. N. G.; Halim, M.; Lupton, J. M.; Burn, P. L.; Samuel, I. D. W. *Macromolecules* **1999**, *32*, 5985.

(7) Lupton, J. M.; Samuel, I. D. W.; Burn, P. L.; Mukamel, S. *J. Phys. Chem. B.* **2002**, *106*, 7647.

(8) Lee, M.; Park, M.-H.; Oh, N.-K.; Zin, W.-C.; Jung, H.-T.; Yoon, D. K. *Angew. Chem., Int. Ed* **2004**, *43*, 6465.

(9) Yoon, D. K.; Lee, S. R.; Lee, E. H.; Kim, Y. H.; Choi, S.-M.; Jung, H.-T. *Adv. Mater.* **2006**, *18*, 509.

(10) (a) Kim, J.; Swager, T. M. *Nature* **2001**, *411*, 1030. (b) Han, J. T.; Zheng, Y.; Cho, J. H.; Xu, X.; Cho, K. *J. Phys. Chem. B.* **2005**, *109*, 20773.

(11) Shklyarevskiy, I. O.; Jonkheijm, P.; Stutzmann, N.; Wasserberg, D.; Wondergem, H. J.; Christianen, P. C. M.; Schenning, A. P. H. J.; de Leeuw, D. M.; Tomovic, Z.; Wu, J.; Mullen, K.; Maan, J. C. *J. Am. Chem. Soc.* **2005**, *127*, 16233.

(12) Swiggers, M. L.; Xia, G.; Slinker, J. D.; Gorodetsky, A. A.; Malliaras, G. G.; Headrick, R. L.; Weslowski, B. T.; Shashidhar, R. N.; Dulcey, C. S. *Appl. Phys. Lett.* **2001**, *79*, 1300.

(13) Xu, L.-P.; Yan, C.-J.; Wan, L.-J.; Jiang, S.-G.; Liu, M.-H. *J. Phys. Chem. B.* **2005**, *109*, 14773.

(14) Percec, V.; Glodde, M.; Bera, T. K.; Miura, Y.; Shiyanovskaya, I.; Singer, K. D.; Balagurusamy, V. S. K.; Heiney, P. A.; Schnell, I.; Rapp, A.; Spiess, H.-W.; Hudson, S. D.; Duank, H. *Nature* **2002**, *419*, 384.

(15) Shiyanovskaya, I.; Singer, K. D. *Phys. Rev. B* **2003**, *67*, 535204.

(16) (a) Masuo, S.; Yoshikawa, H.; Asahi, T.; Masuhara, H. *J. Phys. Chem. B* **2003**, *107*, 2471. (b) Sato, T.; Jiang, D.-L.; Aida, T. *J. Am. Chem. Soc.* **1999**, *121*, 10658.

(17) Henderson, P.; Beyer, D.; Jonas, D.; Jonas, U.; Karthaus, O.; Ringsdorf, H.; Heiney, P. A.; Miliszewskyj, N. C.; Ghosh, S. S.; Mindyuk, O. Y.; Josefowicz, J. Y. *J. Am. Chem. Soc.* **1997**, *119*, 4740.

(18) Yang, Y.; Yan, H.; Fu, Z.; Yang, B.; Xia, L.; Xu, Y.; Zuo, J.; Li, F. *J. Phys. Chem. B.* **2006**, *110*, 846.

(19) Hoogboom, J.; Garcia, P. M. L.; Otten, M. B. J.; Elemans, J. A. A. W.; Sly, J.; Lazarenko, S. V.; Rasing, T.; Rowan, A. E.; Roeland J. M. *J. Am. Chem. Soc.* **2005**, *127*, 31.

(20) Percec, V.; Johansson, G.; Ungar, G.; Zhou, J. *J. Am. Chem. Soc.* **1996**, *118*, 9855.

(21) Lee, E. H.; Yoon, D. K.; Jung, J. M.; Lee. S. R.; Kim, Y. H.; Kim, Y.-A.; Kim, G. C.; Jung, H.-T. *Macromolecules* **2005**, *38*, 5152.

(22) Percec, V.; Cho, W.-D.; Ungar, G. *J. Am. Chem. Soc.* **2000**, *122*, 10273.

(23) Winnik, F. M. *Chem. Rev.* **1993**, *93*, 587.

(24) Wang, W.; Han, J. J.; Wang, L. Q.; Li, L. S.; Shaw, W. J.; Li, A. D. Q. *Nano Lett.* **2003**, *3*, 455.

(25) (a) Zucolotto, V.; Faceto, A. D.; Santos, F. R.; Mendonca, C. R.; Guimaraes, F. E. G.; Oliveira, O. N., Jr. *J. Phys. Chem. B* **2005**, *109*, 7063. (b) Ye, K.; Wang, J.; Sun, H.; Liu, Y.; Mu, Z.; Li, F.; Jiang, S.; Zhang, J.; Zhang, H.; Wang, Y.; Che, C.-M. *J. Phys. Chem. B.* **2005**, *109*, 8008.

(26) Kim, J.; McQuade, D. T.; McHugh, S. K.; Swager, T. M. *Angew. Chem., Int. Ed.* **2000**, *39*, 3868.

(27) Wu, J.; Fechtenkotter, A.; Gauss, J.; Watson, M. D.; Kastler, M.; Fechtenkotter, C.; Wagner, M.; Mullen, K. *J. Am. Chem. Soc.* **2004**, *126*, 11311.
(28) Ferguson, J. J. *Chem. Phys.* **1958**, *28*, 765.
(29) Klessinger, M.; Michel, J. *Excited States and Photochemistry of Organic Molecules*; VCH: New York, 1995.
(30) Langhals, H.; Ismael, R. *Eur. J. Org. Chem.* **1998**, *9*, 1915.
(31) Jung, H.-T.; Kim, S. O.; Ko, Y. K.; Yoon. D. K. *Macromolecules* **2002**, *35*, 3717.
(32) (a) Lee, S. R.; Yoon, D. K.; Park, S. H.; Lee, E. H.; Kim, Y. H.; Stenger, P.; Zasadzinski, J. A.; Jung, H.-T. *Langmuir* **2005**, *21*, 4989. (b) Yoon, D. K.; Jung, H.-T. *Langmuir* **2003**, *19*, 1123.